A Damage Accumulation Model of Fatigue Crack Growth in Titanium

Carlos A. R. P. Baptista[1] and Viktor A. Pastoukhov[2]

[1]*FAENQUIL/Demar - Department of Materials Engineering, Polo Urbo-Industrial, Gleba AI-6, C.P. 116,CEP 12600-000, Lorena/SP, Brazil – baptista@demar.faenquil.br.*

[2]*Department of Mathematics and Physics, Universidade de Taubaté (UNITAU), Taubate/SP, currently with EMBRAER – Empresa Brasileira de Aeronáutica S.A., CEP 12227-901, São Jose dos Campos/SP, Brazil – viktor.pastoukhov@embraer.com.br*

ABSTRACT

This work introduces a predictive method in which the fatigue crack propagation is treated in terms of cumulative damage of volume elements along the crack path. The development of the work includes considerations about the stress distribution in the cracked body and the stress-life and strain-life relations to be used in the computational procedure. It is assumed that the scattering of the stress-life data can be reproduced in the volume elements ahead of the crack, thus allowing probabilistic predictions to be performed. In order to check the reliability of the model, constant amplitude fatigue crack growth tests with load ratios of R = 0.1 and R = 0.5 were carried out in two sets of 15 commercial purity titanium sheet samples and the results were compared to the computational simulations.

Key words: fatigue crack propagation, cumulative damage, fracture mechanics, titanium.

1. INTRODUCTION

The study of fatigue crack propagation (FCP) is aimed at residual life estimations in order to apply the fail-safe criterion. Usual approaches include the concepts of fracture mechanics in the form of semi-empirical models based on the well-known "Paris law" of FCP /1/, which considers the stress intensity range, ΔK, as the governing driving force for crack growth. However, these models can lead to a weak correlation between predictions and the actual lifetime of components. Although the crack closure concept /2/ explains some effects, like variations on crack growth rate due to load ratio, the difficulties inherent to its measurement inhibit its employment in a wide range of situations /3/. A unified approach /4/ was proposed, in which load ratio effects were recognized as intrinsic to fatigue. Thus, the load dependence arises because of the presence of two driving forces for fatigue: one represented by the stress intensity range and the other by the peak stress intensity factor, K_{max}.

Despite these improvements, a significant restriction to this methodology is related to the prediction of the material's behavior in a wide range of actual loading conditions, as well as in the presence of variable amplitude loading. Furthermore, it is known that most metallic materials have a polycrystalline microstructure of random orientation, described by various parameters, which may seriously affect crack growth. As a result, the deterministic theories of FCP could be accepted only as an approximation of the phenomenon /5-7/.

On the other hand, the local approach of fracture /8/, in the framework of damage mechanics, may point at a way to overcome such limitations. In this case, the crack is considered as a set of representative volume elements in which critical damage conditions were achieved. Various predictive models of FCP were proposed, using different failure criteria, e.g. absorbed energy /9/ and low cycle fatigue data /10/. Although they have not achieved a reliability level high enough to be used in design, these models allow for the intelligent ranking of alloy systems in terms of fatigue crack growth resistance prior to a more specific fracture mechanics documentation of the selected system. However, there is a lack in the development of stochastic cumulative damage models /11/, due mainly to the scarcity of experimental data for the validation of such models.

The aim of this work is to develop a predictive model of FCP that considers the growth of a main crack as a sequence of failures of damage accumulating volume elements along the crack path. Considerations about the stress distribution in the cracked body and the stress-life and strain-life relations to be used in the computational procedure are included. It is assumed that the scattering of the stress-life data can be reproduced in the volume elements ahead of the crack, thus allowing probabilistic predictions to be performed. In order to check the reliability of the model, constant amplitude fatigue crack growth tests with load ratios of R = 0.1 and R = 0.5 were carried out in two sets of 15 commercial purity titanium (ASTM grade II) sheet samples and the results were compared to the computational simulations.

2. MODELLING SCHEME

The modelling of fatigue crack growth by methods of continuum damage mechanics is based on three main keystones: analysis of stress and strain in the cracked body; equation of lifetime reduction as a function of the stress-strain state and crack advance criterion. In this work, a method for the stress analysis ahead of the crack is proposed. The stress and strain-life relations are obtained from basic fatigue data and the linear rule of damage summation is assumed. The fatigue state is described by a scalar damage parameter d, whose value changes from 0 (undamaged state) to 1 (final fracture). The damage accumulation process is not restricted to the cyclic plastic zone.

2.1 Stress field ahead of the crack

The available analytical expression for a mode I crack, given by Eq. (1), is based on the elastic asymptotic deduced for an infinite plate and valid only in the neighbourhood of the crack tip /12/. In this expression, K_I is the stress intensity factor, as shown by Eq. (2), and r is the distance from the crack tip.

$$\sigma_{as}(r) = \frac{K_I}{\sqrt{2\pi r}} \quad (1)$$

$$K_I = G(\lambda)\sigma_0\sqrt{\pi a} \quad (2)$$

where σ_0 is the stress in the uncracked section, G is a geometric function in which the parameter λ is defined as $\lambda = a / w$ for plane cracked specimens whose width is w.

The plastic zone, as defined by Irwin /13/ or Dugdale /14/, limits the stress on the singularity represented by the crack tip, but it does not take into account the finite width of the body and its effect on the stress distribution far from the crack. In order to achieve a better description of the stress field ahead of the crack, an analytical expression is proposed, based on the numerical analysis performed by the finite element method (computer program ANSYS®), which showed a smooth transition between the classical asymptotic near the crack and the external load level along the side boundaries of the sample. Moreover, this approach of the stress distribution is based on the fundamental hypotheses of continuity and equilibrium, and was developed in two steps. For the first step, a purely elastic material was assumed, and the stress distribution normal to the crack path is given by:

$$\sigma(r) = \sigma_0 + \sigma_{as}(r)\left[1 - \left(\frac{r}{w-a}\right)^m\right] \quad (3)$$

where m is an adjustment parameter.

The parameter m is calculated by imposing the equilibrium condition given by Eq. (4). The solution for m can be written as Eq. (5), in which m^* is given by Eq. (6), showing that m is a function of λ.

$$w\sigma_0 = \int_0^{w-a} \sigma(r)dr \quad (4)$$

$$m = \frac{m^*}{\left(4 - 2m^*\right)} \quad (5)$$

$$m^* = \frac{\lambda\sqrt{2}}{G(\lambda)\sqrt{\lambda(1-\lambda)}} \quad (6)$$

The second step considers a limiting value for the stress, σ_l, in order to take into account the crack tip plasticity. Hence, the stress distribution is described by the expressions given below, in which r_p is the plastic zone size and φ is a local-stress coefficient.

$$\sigma(r) = \begin{cases} \sigma_l, & 0 \le r \le r_p \\ \sigma_0 + \varphi\sigma_{as}(r)\left[1 - \left(\dfrac{r}{w-a}\right)^m\right], & r \ge r_p \end{cases} \tag{7}$$

An expression for φ is obtained making $r = r_p$ and equalizing both parts of the function $\sigma(r)$ given in Eq. (7). If β and ψ are defined according to Eqs. (8) and (9), then φ can be written in terms of β, λ and ψ, as shown in Eq. (10).

$$\beta = \frac{r_p}{w} \tag{8}$$

$$\psi = \frac{\sigma_0}{\sigma_l} \tag{9}$$

$$\varphi = \frac{(1-\psi)\sqrt{2\beta}}{\psi G(\lambda)\sqrt{\lambda}\left[1 - \left(\dfrac{\beta}{1-\lambda}\right)^m\right]} \tag{10}$$

The equilibrium condition given by Eq. (4) is then imposed to Eq. (7), leading to:

$$\psi(\lambda+\beta) - \beta - \frac{\varphi G(\lambda)\psi\sqrt{\lambda}}{\sqrt{2}}\left[m^*\sqrt{1-\lambda} - 2\sqrt{\beta} + \frac{\beta^{m+0.5}}{(m+0.5)(1-\lambda)^m}\right] = 0 \tag{11}$$

Equation (11) defines a function $f(\beta) = 0$, whose solution, that is, the value of β is obtained numerically, e.g. by the bisection method. In order to use this calculation procedure when a cyclic loading is considered, σ_{max} (maximum stress of the load cycle) is adopted as σ_0. The unloading stress distribution is calculated by subtracting the elastic stress distribution corresponding to σ_{min} (minimum stress of the load cycle) from $\sigma(r)$. The first one is obtained by multiplying Eq. (7) by *(1 - R)*. Also in this case, it is necessary to limit the minimum stress by $-\sigma_l$, defining the cyclic plastic zone.

2.2 Discretization of the cracked body

In order to simulate FCP from an initial size a_0, a linear path is assumed, which is discretized in a set of t elementary steps with length da. Each one of these steps corresponds to a material's volume element whose stress-strain state is considered as uniform. The maximum stress of a load cycle in the volume element number i after the failure of j elements is written as $\sigma_{i,j}$, as shown in Fig. 1, and the corresponding stress ratio is $R_{i,j}$.

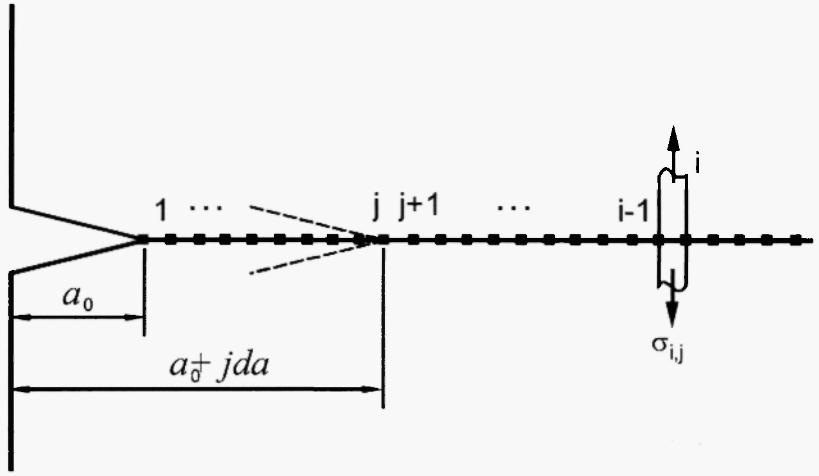

Fig. 1: Discretization of the cracked body.

2.3 Probabilistic criterion

The discretization procedure allows for the performance of computer simulations of FCP. In each simulation, a random number generator is employed with the Monte Carlo technique in order to attribute to each volume element a deviation parameter x_i. This parameter is related to the statistical distribution of fatigue life curves obtained from smooth specimens, as shown in a previous work /15/. Thus, each set of x_i values ($i = 1, ..., t$) leads to a different crack growth history under the same loading regime.

2.4 Algorithm of FCP calculation

After the initial conditions are established, the logarithimic number of cycles to fracture of the first volume element is calculated using an appropriate function of the stress-strain state, $f(\sigma, R)$, in the following form:

$$n_1 = log(N_1) = f(\sigma_{1,0}, R_{1,0})(1 + x_1) \quad (12)$$

The damage accumulated in the remaining elements during this period is given by:

$$d_{i,1} = 10^{\left[n_1 - f\left(\sigma_{i,0}, R_{i,0}\right)\left(1+x_i\right)\right]}, \tag{13}$$

for $i = 2, ..., t$.

The logarithmic number of cycles to each crack increment, Δn_j, corresponds to the accumulation of critical damage in the subsequent volume element, beginning from the damage already accumulated under the previous increments. According to the linear rule of damage summation, one has:

$$d_{j,j} = 1 - \sum_{l=1}^{j-1} d_{j,l} \tag{14}$$

leading to:

$$\Delta N_j = d_{j,j} 10^{f\left(\sigma_{j,j-1}, R_{j,j-1}\right)\left(1+x_j\right)} \tag{15}$$

During this period, the remaining elements accumulate the damage:

$$d_{i,j} = 10^{\left[\Delta n_j - f\left(\sigma_{i,j-1}, R_{i,j-1}\right)\left(1+x_i\right)\right]}, \tag{16}$$

for $i = (j + 1), ..., t$.

The process is repeated until the total failure of the cracked element.

3. MATERIAL PROPERTIES

Commercially pure (ASTM grade II) titanium was chosen for this work. The basic mechanical properties of this material are the following: Yield strength σ_{ys} = 349 MPa, ultimate tensile strength σ_u = 488 MPa, Young's modulus E = 102.7 GPa, elongation to fracture ΔL = 26.6%.

The cyclic stress-strain curve at room temperature is given by Eq. (17) /16/.

$$\sigma_a = 379\left(100\varepsilon_a\right)^{0.4} \tag{17}$$

where σ_a is the stress amplitude and ε_a is the total strain amplitude.

By means of low cycle fatigue tests of grade II titanium samples /17/, the Coffin-Manson equation was determined, as shown below:

$$\varepsilon_{ap} = 0.083(2N)^{-0.42} \tag{18}$$

where ε_{ap} is the plastic strain amplitude and *2N* is the number of reversals to fracture.

The Morrow-Landgraf approach /18, 19/ was adopted in order to describe the fatigue behavior under different stress ratios. A numerical regression was made from experimental stress-life data obtained from smooth samples /20/, leading to:

$$2N = \left[\frac{\sigma_{max}(1-R)}{1397 - \sigma_{max}(1+R)} \right]^{-10.408} \tag{19}$$

where σ_{max} is the maximum stress of the load cycle and R is the stress ratio.

4. NUMERICAL SIMULATIONS

Computer simulations of FCP under constant-amplitude loading were performed. The discretized domain simulated a center-notched specimen with 50 mm in width. Two load ratios were adopted: R = 0.1 and R = 0.5. For each one, 15 FCP curves starting from an initial crack size a_0 = 7.5mm were generated.

The computer program used Eq. (7) for calculation of the stress field ahead of the crack, where the coordinate of the volume element number *i* after the fracture of *j* elements is given by:

$$r = (i - j)da \tag{20}$$

The so-called effective yield strength, given by Eq. (21), was adopted as the value for σ_l.

$$\sigma_l = \frac{(\sigma_{ys} + \sigma_u)}{2} \tag{21}$$

In order to specify the functions $f(\sigma, R)$ used by Eqs. (12), (13), (15) and (16), the material ahead of the crack is divided into three parts, as shown in Fig. 2. For the cyclic plastic zone ($r \leq r_c$), R = -1 and the Coffin-Manson approach is adopted. In this case, Eq. (17) is used to calculate the total strain amplitude from which the plastic strain is obtained. If $r_c < r \leq r_p$, the Morrow-Landgraf approach is adopted and thus Eq. (19) is used. Beyond the plastic zone ($r > r_p$), S/N curves can be used when available, remembering that it is also possible to adopt the Morrow-Landgraf approach in this case.

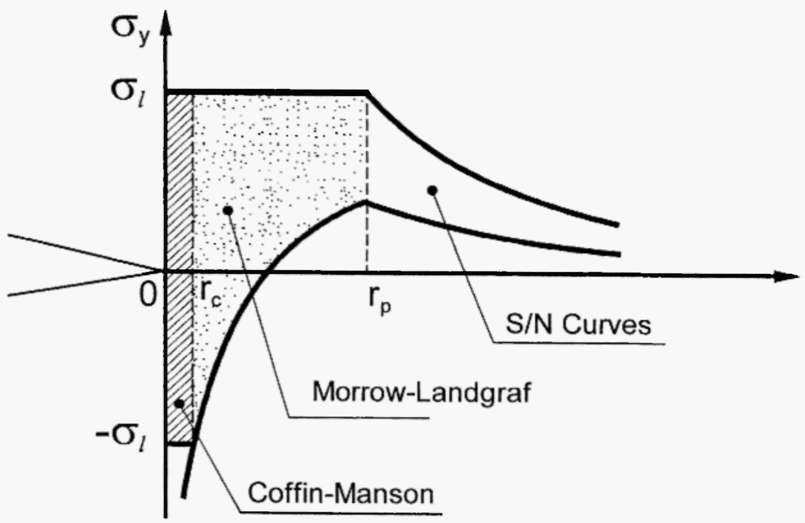

Fig. 2: Stress diagrams and the adopted fatigue life approaches.

5. EXPERIMENTAL PROCEDURE

Fatigue crack growth tests of the titanium sheet (thickness = 1.5 mm) samples were performed in a MTS servo-hydraulic machine under conditions similar to those adopted for the computer simulations. Stationary cyclic loading (frequency = 10 Hz) was applied, the maximum load in a cycle being 8.0 kN. A number of 30 center-notched specimens (width = 50 mm, notch length = 12 mm) were tested, 15 of them with a load ratio R = 0.1 and the other 15 with R = 0.5. Initial crack measurements were made from a total crack length of $2a_0$ = 15 mm. Crack size was measured using a travelling microscope (precision = ± 0.01 mm).

6. COMPARISON OF RESULTS

The results of the numerical simulations were found to depend on the discretization step *da*. Thus, a value for *da* was chosen, small enough to lead the numerical simulations for both R-ratios to reasonable and stable results. This value was $da = {}^{1}/_{75}$ mm. The numerical results are given in plots of "crack length *versus* number of cycles", as shown in Figs. 3 and 4. The experimental results of FCP tests are presented in the same manner in Figs. 5 and 6. The simulated and experimental curves have similar shapes, although simulations present the serrate feature typical for discrete procedures.

Tables 1 and 2 allow for analysis of the numerical results when compared to experiments. These tables present the mean values (μ), standard deviation (SD) and coefficient of variation (C_v) corresponding to 2.5 mm intervals of crack growth. It can be seen that the simulations predict an initial crack growth faster than

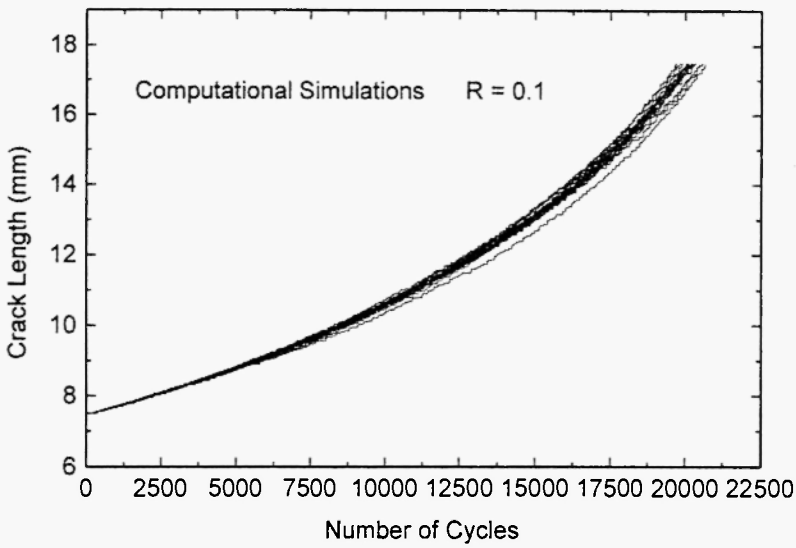

Fig. 3: Numerical simulations of FCP, R = 0.1.

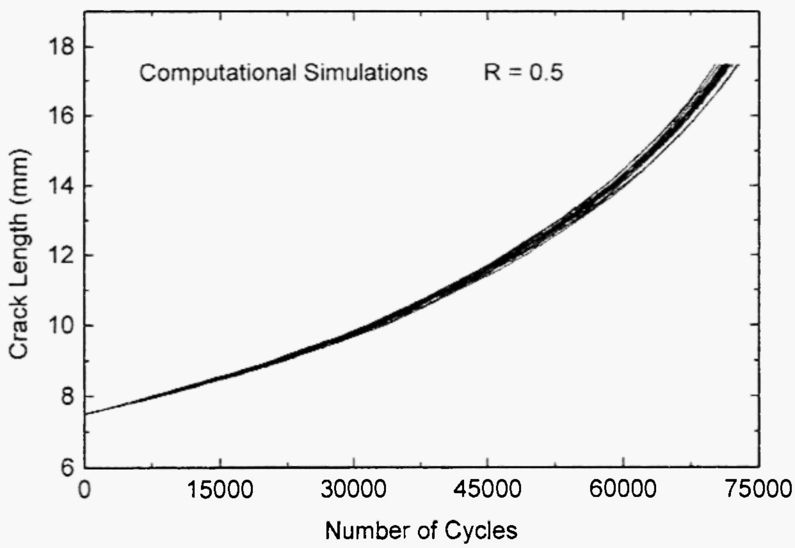

Fig. 4: Numerical simulations of FCP, R = 0.5.

the tests, and this tendency is inverted in the second half of the curves. This may indicate that it is necessary to perform a more detailed consideration of the complex stress state on the volume elements, leading to calculations of equivalent stresses. However, the predicted number of cycles to achieve the critical crack length is very close to the experimental results, especially if the intervals defined by the standard deviation

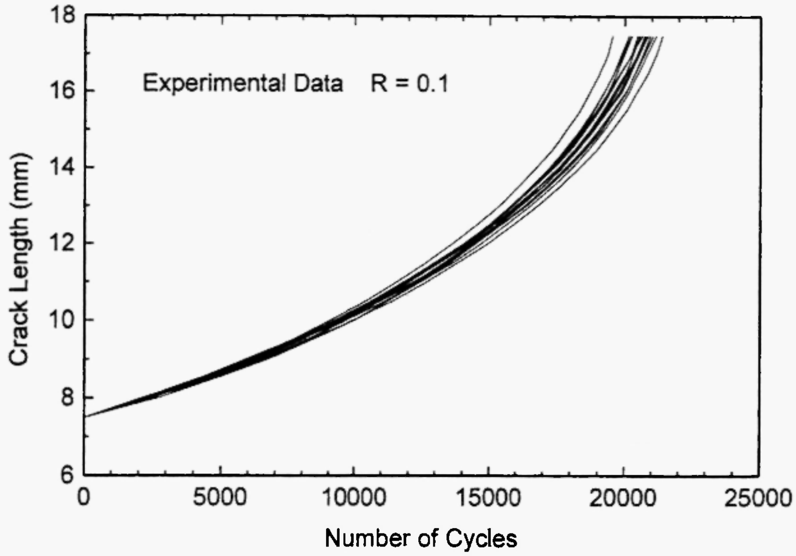

Fig. 5: Experimental results, R = 0.1.

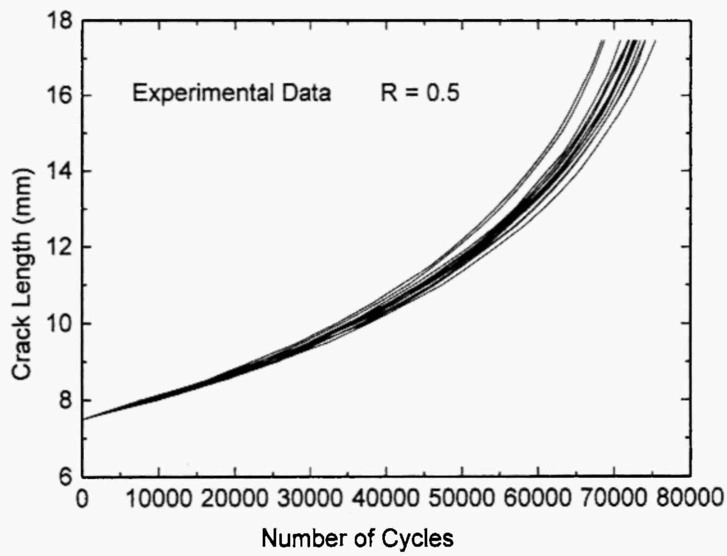

Fig. 6: Experimental results, R = 0.5.

are considered.

Besides, Tables 1 and 2 show that the predicted scattering is lower than that observed in the experiments. One possible reason for this behaviour is due to the drawing technique employed for the deviation parameter x. It is known, for example, that if a crack starts growing faster than the average, this tendency is maintained

Table 1

Comparison of results for R = 0.1

Interval (mm)	Simulations		Tests	
	$\mu \pm$ S.D.	C_V (%)	$\mu \pm$ S.D.	C_V (%)
7.5 → 10.0	8588 ± 207	2.41	9485 ± 245	2.58
10.0 → 12.5	5373 ± 113	2.10	5731 ± 129	2.25
12.5 → 15.0	3687 ± 101	2.74	3519 ± 108	3.06
15.0 → 17.5	2539 ± 112	4.41	1910 ± 119	6.25

Table 2

Comparison of results for R = 0.5

Interval (mm)	Simulations		Tests	
	$\mu \pm$ S.D.	C_V (%)	$\mu \pm$ S.D.	C_V (%)
7.5 → 10.0	32419 + 536	1.65	36144 ± 1395	3.86
10.0 → 12.5	18668 ± 292	1.56	19213 ± 618	3.22
12.5 → 15.0	12378 ± 240	1.94	10901 ± 232	2.13
15.0 → 17.5	8273 ± 179	2.16	6192 ± 254	4.10

during the test. Thus, the value of parameter x, for a given volume element should not be fully independent of the previous elements. Although the drawing of the deviation parameters by the Monte Carlo technique reproduces the scattering parameters of the fatigue life, this local dependency is ignored, reducing the scattering of the simulated FCP curves.

7. CONCLUSIONS

The modelling approach developed in this work allowed the obtaining of probabilistic calculations of FCP, based on the scattering of the fatigue life data for titanium smooth specimens. Considerations about equilibrium and the finite width of the body lead to a new equation describing the stress field ahead of the crack, which is in accordance with FEM calculations. Experimental results of the crack growth tests in commercial purity titanium showed good agreement with those obtained from computer simulations for the adopted conditions. These results show that it is possible to obtain reasonable predictions of crack growth without previous knowledge of FCP data, although a certain dependence on the discretization step was observed. Further improvements may include generalizations for damage accumulation model, as well as for stress-strain behaviour of the material. Other materials should also be investigated, in order to check the proposed model.

8. ACKNOWLEDGEMENTS

The authors are thankful to CTA/IAE/AMR (São Jose dos Campos/SP/Brazil) and to FAPESP (proc. 98/15048-8).

9. REFERENCES

1. P. Paris and F. Erdogan. A critical analysis of crack propagation laws. *J. Basic Engng, Trans. ASME*, 528-534 (1963).
2. W. Elber. The significance of fatigue crack closure. In: *Damage Tolerance in Aircraft Structures*, ASTM STP 486, Philadelphia, PA, 1971; pp. 230-247.
3. N. Louat, K. Sadananda, M. Duesbery and A.K. Vasudevan. A theoretical evaluation of crack closure. *Metall. Trans. A*, **24A**, 2225-2232 (1993).
4. K. Sadananda and A.K. Vasudevan. Unified approach to fatigue crack growth. In: *Proc. of International Conference on Mechanical Behaviour of Materials*, Victoria, Canada, Vol. 1, 1999; pp.283-288.
5. D.A. Virkler, B.M. Hillberry and P.K. Goel. The statistical nature of fatigue crack propagation. *Trans. ASME*, **101**, 148-153 (1979).
6. K. Ortiz and A.S. Kiremidjian. Stochastic modelling of fatigue crack growth. *Engng Fract. Mech.*, **29**, 317-334 (1988).
7. C. Lapetra, J. Mayo and J. Domínguez. The randomness of fatigue crack growth under constant-amplitude loads. *Fatigue Fract. Engng Mater. Struct.*, **19**, 589-600 (1996).
8. J. Lemaitre. Local approach of fracture. *Engng Fract. Mech.*, **25**, 532-537 (1986).
9. R.P. Skelton, T. Vilhelmsen and G.A. Webster. Energy criteria and cumulative damage during fatigue crack growth. *Int. J. Fatigue*, **20**, 641-649 (1998).
10. J.R. Durán, J.T.P. Castro and M.A. Meggiolaro. A damage accumulation model to predict fatigue crack growth under variable amplitude loading using εN parameters. In: *Proc. of the Eighth International Fatigue Congress*, Stockholm, Sweden, Vol. 2, 2002; pp.1451-1458.

11. B. Bhattacharya and B. Ellingwood. Continuum damage mechanics-based model of stochastic damage growth. *Journal of Engineering Mechanics, ASCE*, **124**, 1000-1009 (1998).
12. H.L. Ewalds and R.J.J. Wanhill. *Fracture Mechanics*. Edward Arnold & Delftse Vitgevers Maatschappij, London, 1986.
13. G.R. Irwin (1960) Plastic zone near a crack and fracture toughness. In: *Proc. of 7th Sagamore Mater. Conf.*, Syracuse Univ. Press, 1960.
14. D. S. Dugdale. Yielding of steel sheets containing slits. *J. Mech. And Phys. Solids*, **8**, 100-108 (1960).
15. C.A.R.P. Baptista, V.A. Pastoukhov, E.M.R. da Silva and A.F. Siqueira. Probabilistic predictions of fatigue crack behaviour. In: *Proc. of Boundary Element Technology and International Conference on Computer Methods and Testing for Engineering Integrity*, Las Vegas, USA, 1999; pp.539-548.
16. J.I. Dickson, J. Ducher and A. Plumtree. Cyclic behavior and delayed softening of commercial purity titanium. *Metall. Trans. A*, **7**, 1559-1565 (1976).
17. X.P. Song, G.L. Chen and H.C. Gu. Low cycle fatigue behavior of commercial purity titanium in liquid nitrogen. *Int. J. Fatigue*, **24**, 49-56 (2002).
18. M. Klesnil and P. Lukás. *Fatigue of Metallic Materials*. Elsevier, Amsterdam, 1992.
19. R. W. Landgraf. The resistance of metals to cyclic deformation. In: *Achievement of High Fatigue Resistance in Metals and Alloys*, ASTM STP 467, Philadelphia, PA, 1970; pp.3-36
20. E.M.R. da Silva. Investigation of Cumulative Fatigue Damage in Titanium. Master thesis, DEMAR/FAENQUIL, Engineering College of Lorena, Brazil, 1998; 103p.